

Electronic properties of domain walls in $\text{La}_{2/3}\text{Sr}_{1/3}\text{MnO}_3$: Magnetotransport measurements on a nanopatterned device

T. Arnal,¹ A. V. Khvalkovskii,² M. Bibes,¹ B. Mercey,³ Ph. Lecoeur,¹ and A.-M. Haghiri-Gosnet¹

¹*Institut d'Electronique Fondamentale, CNRS, Université Paris-Sud, 91405 Orsay, France*

²*General Physics Institute of the Russian Academy of Science, Vavilova Street 38, 119991 Moscow, Russia*

³*CRSIMAT-ISMRA, 6 Boulevard du Maréchal Juin, 14050 Caen Cedex, France*

(Received 22 March 2007; revised manuscript received 2 May 2007; published 29 June 2007)

Domain walls (DWs) in strongly correlated ferroics are expected to exhibit rich physical properties due to the competition between ground states that exists in these systems. A typical example is provided by ferromagnetic mixed-valence manganites for which insulating DWs in an otherwise metallic phase have been predicted. Through magnetotransport experiments on a nanopatterned device we have determined the electronic properties of DWs in $\text{La}_{2/3}\text{Sr}_{1/3}\text{MnO}_3$. We find a DW resistance-area (RA) product of $\sim 2.5 \times 10^{-13} \Omega \text{ m}^2$ at low temperature and bias, which is several orders of magnitude larger than the values reported for 3d ferromagnets. However, the current-voltage characteristics are highly linear, which indicates that the DWs are not phase separated but metallic. Remarkably, the DWRA is also found to increase upon increasing the injected current, presumably reflecting some deformation of the wall by spin transfer.

DOI: [10.1103/PhysRevB.75.220409](https://doi.org/10.1103/PhysRevB.75.220409)

PACS number(s): 75.60.Ch, 75.47.Lx

The physics of domain walls (DWs) in ferroic materials has become a subject of great focus over the recent years. While most early works were on DWs in ferromagnetic materials,¹ some recent (experimental and theoretical) papers have actually addressed the question of the properties of DWs in other ferroic systems such as ferroelectrics² or ferroelastics.³ Indeed, it was recently pointed out that there exist general scaling laws that relate the domain and domain wall widths to the film thickness in ferromagnets, ferroelectrics, and even relaxors.⁴

Besides these general trends, much remains to be understood on the detailed nanoscale physical properties of DWs. This is particularly true in strongly correlated systems because the general theory that relates the width of a wall in a ferromagnet to exchange and anisotropy⁵ ignores correlation effects. This problem was first addressed theoretically by Mathur and Littlewood in a paper dealing with phase instability in manganites.⁶ Such Mn oxides have a very rich phase diagram, with competing insulating and metallic phases, that are usually antiferromagnetic and ferromagnetic, respectively.⁷ Under certain conditions, the perturbation caused by the presence of a DW in a metallic-ferromagnetic manganite would drive a transition to an insulating phase inside the wall.^{6,8,9} The wall would then be phase separated, and phase separation is indeed a wide spread phenomenon in manganites.¹⁰ Therefore manganites appear as a model system to study the possible existence of DWs with inhomogeneous electronic properties, beyond Kittel's theory.

Little is known on magnetic DWs in manganites.^{11,12} Fresnel imaging has been used to measure the width δ of a DW in a 200 nm $\text{La}_{2/3}\text{Ca}_{1/3}\text{MnO}_3$ (LCMO) film, yielding $\delta \approx 38$ nm.¹³ Their contribution to the resistance was measured in patterned LCMO strips and a resistance-area (RA) product of $8 \times 10^{-14} \Omega \text{ m}^2$ was found at 77 K (Ref. 11), which is several orders of magnitude larger than what is found in Co or NiFe (Ref. 14). Estimations based on a simple application of the double-exchange model revealed that the resistivity increase due to conventional Bloch-type DWs^{11,15} cannot possibly explain experimental results.

To gain more insight on the electronic properties of DWs in manganites, we have fabricated devices consisting of a strip with nanometric notches in a $\text{La}_{2/3}\text{Sr}_{1/3}\text{MnO}_3$ (LSMO) epitaxial thin film. In the magnetic field (H) dependence of the resistance (R) of these devices, we observe jumps at low magnetic field that we attribute to DWs. Significantly, we have found that even though the resistance of these DWs is indeed very large, we do not observe any of the signatures that one might expect if DWs were actually phase separated. In addition, we have found that the DW resistance increases with increasing the injected current. We discuss this result in terms of spin-transfer torque effects and the modification of the local electronic structure of the LSMO at the notches.

LSMO thin films (thickness $t=10$ nm) were grown on (001)-oriented SrTiO_3 (STO) substrates by pulsed laser deposition. The films are epitaxial as evidenced by x-ray diffraction studies, and their surface shows flat terraces separated by one-unit-cell-high steps. The grain size is typically $\sim 100 \mu\text{m}$. The Curie temperature (T_C) of the films was 320 K, i.e., slightly lower than the bulk T_C (360 K) due to their low thickness.¹⁶ $M(H)$ cycles measured at 10 K along different in-plane directions evidenced a biaxial anisotropy, with the easy axes along [110] and $[-110]$ (Ref. 17). The corresponding cubic anisotropy constant was $K = -9 \times 10^3 \text{ J m}^{-3}$.

The films were patterned by electron-beam lithography, using a negative resist HSQ-FOX 12. No subsequent annealing was applied. The exposure was performed in a modified field-effect gun scanning electron microscopy (SEM) at 30 keV (see Ref. 17 for details). The strip was oriented along the easy [110] direction. After exposure, development, and ion-beam etching, the ~ 100 -nm-thick (insulating) resist was left on the patterned strip, although its thickness was strongly reduced at the notches. The devices defined with this process consist of a 350-nm-wide and 2- μm -long central domain connected on each side to 1- μm -wide and 15- μm -long strips by two narrow notches. Figure 1(a) shows a SEM image of one of the devices. Atomic force microscopy (AFM) images

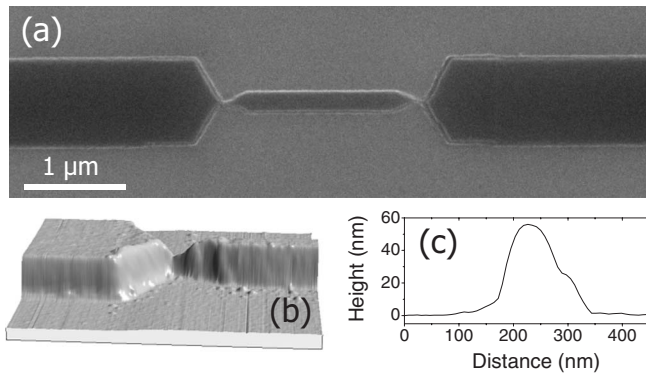


FIG. 1. (a) Scanning electron microscopy image of the device, i.e., the LSMO strip covered by the resist, after ion beam etching. (b) AFM image of one of the notches. (c) Profile across one of the notches.

[Fig. 1(b)] and cross sections [Fig. 1(c)] of the notches revealed that their width is 100–150 nm. Micronic sputtered Au pads were used as contacts.

The dimensions of the devices were determined in view of micromagnetic simulations results and chosen so as to allow magnetization reversal in the central region at a larger field than in the outer arms. This is illustrated in Fig. 2 that shows the calculated micromagnetic configuration of the device in the antiparallel state. The simulations were performed by numerical integration of the Landau-Lifshitz equations on a two-dimensional mesh. We took $M_S = 550 \text{ emu cm}^{-3}$ for the saturation magnetization, $A = 3.7 \text{ erg cm}^{-1}$ for the exchange constant (deduced from the spin-stiffness data given in Ref. 18), and the anisotropy parameter given above. The discretization step was 5 nm. Field induced magnetization reversal of the device initially saturated in the opposite direction was simulated. Upon increasing the field, the magnetization in one of the wide arms reverses, then in the second one, and at a certain field DWs of the head-to-head type appear at each notch (see Fig. 2). Upon increasing the field further, these DWs become more constrained. Finally, at some critical field the DWs annihilate each other.

In Fig. 3, we show a set of $R(H)$ curves measured at 8 K with different applied bias voltages for the device of Fig. 1

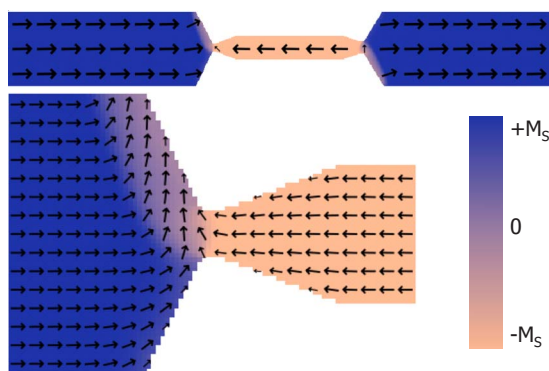


FIG. 2. (Color online) Micromagnetic simulations of the device in the antiparallel configuration with a blowup close to one of the notches.

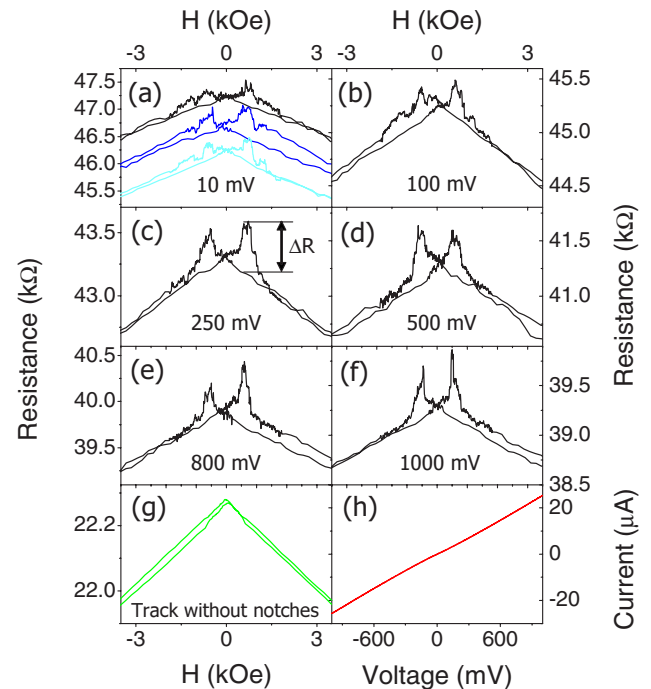


FIG. 3. (Color online) (a)–(f) $R(H)$ curves of the device of Fig. 1 at 8 K and different bias voltages. In (a) the different curves (shifted vertically for clarity) correspond to successive $R(H)$ measurements at 10 mV. (g) $R(H)$ of a strip without notches at 8 K, 100 mV, and with the field applied in-plane and perpendicular to the strip direction. (h) Current-voltage characteristic of the device of Fig. 1 at 8 K.

(sweep rates: ~ 100 and 16 Oe/s at high and low field, respectively). When coming from high positive magnetic field to low negative H values a jump ΔR occurs in the resistance (between -100 and -500 Oe). Upon increasing the field further to large negative values, R shows some sharp features and then recovers a low-resistance state at about -1 kOe . A virtually symmetric behavior is obtained when going back to large positive fields. These jumps are not observed in a strip without notches.¹⁷ We also note that at large field, the resistance decreases linearly, which reflects some spin disorder. The shape and amplitude of the resistance jumps show some scatter as visible from Fig. 3(a) that presents three successive $R(H)$ curves measured at 10 mV. This probably reflects the presence of a number of pinning centers in addition to the notches, especially within the central region. Indeed, the AFM image shown in Fig. 1(b) evidences that the strip edges are not perfect and present some roughness. However, from the different $R(H)$ curves of Fig. 3 there is a clear tendency toward an increase of the resistance jump amplitude as bias voltage is increased.

We have verified that the typical artifacts that occur in domain wall magnetoresistance (DWMR) measurements¹⁴ cannot explain our data. We have measured the MR of a strip without notches with the field applied in plane and perpendicular to the strip direction, see Fig. 3(g). The $R(H)$ is dominated by a linear negative MR in all the field range, as observed at high field for the device with notches. This indicates that the contribution of anisotropic magnetoresis-

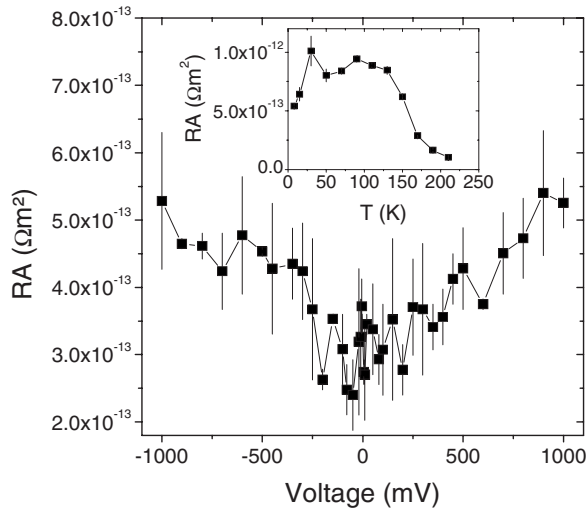


FIG. 4. Bias voltage dependence of the DWRA, at 8 K. Inset: temperature dependence of the DWRA at 900 mV. The error bars correspond to the scatter in the data in successive $R(H)$ runs (when available) or else to the difference in the resistance jump amplitude for positive and negative magnetic field sweep directions.

tance (AMR) is very small. Indeed, for the device with notches, if we assume that in the antiparallel configuration, some fraction of the device (e.g., at the notches) is magnetized perpendicularly to the current direction, we expect the AMR to induce a change in the device resistance of only $\Delta R = R \times \alpha \times f \approx 4 \Omega$ (taking an AMR ratio $\alpha \approx 0.01$ and $f \approx 0.01$ the ratio of the resistance of the notch regions to the total device resistance), which is much smaller than the values observed in Figs. 3(a)–3(f) ($\Delta R \approx 100$ – 500Ω). We also note that the temperature dependence of the DW resistance (see inset of Fig. 4) is different from that of AMR in manganites (see, e.g., Ref. 19). Finally, since our films are magnetized in plane, we can discard the contribution of the Hall effect. We thus conclude that the jumps observed in the $R(H)$ cycles most likely arise from additional carrier scattering due to DWs.

Within this picture, we can calculate the resistance-area product (RA) for the DWs, assuming they are located at the notches. From the value of ΔR and taking a sectional area of $150 \times 10 \text{ nm}^2$, we find that a DW has a RA of $\sim 2.5 \times 10^{-13} \Omega \text{ m}^2$ at 8 K and $|V_{DC}| = 200 \text{ mV}$. This is in good agreement with the value reported by Mathur *et al.*,¹¹ larger by several orders of magnitude than what is found for 3d metals, and about 100 times larger than the DWRA in another ferromagnetic perovskite oxide, SrRuO₃ (Ref. 20). Our results thus confirm that DWs in manganites are highly resistive, with RA values several orders of magnitude larger than what is expected from a simple double-exchange model.¹¹

Further insight into the nature of the DWs can be gained from inspecting the $I(V)$ curves of the device. As visible in Fig. 3(h), they are highly linear, with only a very small nonlinear contribution. This rules out the presence of insulating regions in the strip such as grain boundaries or charge-ordered antiferromagnetic stripes^{6,8,9} that would act as tunnel barriers and thus lead to highly nonlinear $I(V)$ curves. We

thus conclude that our DWs are not of the phase-separated type.^{6,8,9} The very small nonlinear contribution is virtually independent of magnetic field and thus probably reflects the existence of localized states related to structural defects created by the lithography process.

Since our data do not support that phase-separated DWs are responsible for the huge resistance of DWs in LSMO, alternative scenarios must be found. It is known that narrow-band manganites can show a metallic behavior at low temperature and have resistivities of up to $\sim 10^5 \Omega \text{ cm}$, i.e., eight orders of magnitude larger than in LSMO.²¹ While the reduction of the double-exchange interaction due to the rotation of moments within the DW is not enough to explain this large DWRA,¹¹ it is possible that within the DW, the conduction band becomes more narrow due to the reinforced competition between a weakened double-exchange interaction and superexchange. This may lead to a reduced carrier mobility or to the trapping of some carriers as is thought to occur in narrow-band manganites,²¹ hence increasing the resistivity.

The main panel of Fig. 4 shows the variation of the wall resistance with bias voltage. Remarkably, the amplitude of DWRA increases upon increasing the bias voltage (in absolute value) in the -1 to 1 V range. This behavior is qualitatively very different from that observed in manganite-based tunnel junctions, in which the tunnel magnetoresistance (TMR) decreases with bias, under the influence of electron-magnon scattering and band structure effects.²² This further precludes the existence of a charge-ordered antiferromagnetic core in the DWs. The variation of DWRA we observe here is unlikely to be caused by Joule heating, as the device resistance decreases with increasing bias voltage [see Figs. 3(a)–3(f)] while it increases with temperature.¹⁷ However, this possibility cannot be completely ruled out as Joule heating might occur only locally at the notches, which would only yield a small change in the overall device resistance. Besides possible spin-accumulation effects²³ another, most likely, explanation for the bias dependence of DWRA is the deformation of the DW under the influence of the injected current, that is the transfer of spin angular momentum from the spin-polarized current to the local magnetic moment. This spin-pressure effect has been predicted theoretically and experimentally observed at current densities of $J \sim 10^{12}$ – 10^{13} A m^{-2} in NiFe structures.^{24,25} In our case, J is much smaller, on the order of 10^{10} A m^{-2} , but spin torque effects are expected to scale with P/M_S (Ref. 26), which is three times larger in LSMO (taking as spin-polarization $P=0.9$, see Ref. 27) than in NiFe. Furthermore, it is possible that in double-exchange systems, spin-torque effects are more important than in conventional ferromagnets because of the strong on-site Hund interaction that strongly couples the carriers to the local moments. In addition and as previously mentioned, the DWs are very resistive, so that even a small deformation should produce a visible change of DWRA. We point out that this observation suggests rather low critical current densities for domain wall depinning and motion in LSMO, as also found by Pallecchi *et al.*²⁸

The temperature dependence of the DW resistance is shown in the inset of Fig. 4. It increases up to 30 K and then flattens off. Above 125 K it then decreases to vanish around 225 K, which is substantially lower than the T_C of the film

(300 K). In manganites, extrinsic magnetoresistive effects such as powder magnetoresistance²⁹ or TMR³⁰ are known to decrease with temperature and disappear at temperatures lower than T_C . In the case of TMR, this is ascribed to a reduced T_C at the interfaces between the manganite electrodes and the barrier. Here, a possibility would also be that the manganite in the notch regions has a depressed T_C compared to the rest of the film, due to size effects or deterioration by the fabrication process. However, in that case, a signature of the metal-insulator transition (occurring at T_C in manganites³¹) of the notches should have been observed in the $R(T)$ curve that just shows one transition at about 280 K.¹⁷ An alternative mechanism that may account for the DWRA vs T behavior resides in the temperature dependence of the biaxial anisotropy constant in LSMO that decreases rapidly with T and vanishes close to T_C .³² Therefore the DWs are expected to broaden when T increases, which should reduce their contribution to resistance. Temperature dependent magnetic imaging should bring insight to this point.

In summary, we have measured the resistance of magnetic domain walls in a LSMO strip containing two ~ 150 nm

wide notches. We find a DWRA of $2.5 \times 10^{-13} \Omega \text{ m}^2$ at low temperature and bias that increases when increasing the injected current, possibly reflecting the DW deformation by spin transfer. $I(V)$ curves are almost linear which indicates that the DWs in LSMO are not of the phase-separated type despite the strongly correlated nature of LSMO. It is, however, possible that for intermediate- and narrow-band manganites, for which the tendency toward phase separation is stronger,³³ DWs can have an even larger resistance and different electronic properties. Another extension of this work would be to study the current-induced DW motion in half-metallic manganites. Indeed, their large DW resistivities make manganites well-suited for testing DW-based logic architectures with resistive readout.

Financial support by the French ACI Nanomemox, the RFBR project 04-02-17600, and ECONET is acknowledged. We thank B. Montigny for the AFM images, A. Aassime for his help with the lithography process, and K. A. Zvezdin, A. K. Zvezdin, N. D. Mathur, and D. Sánchez for fruitful discussions.

-
- ¹C. H. Marrows, *Adv. Phys.* **54**, 585 (2005).
²P. Paruch, T. Giamarchi, and J.-M. Triscone, *Phys. Rev. Lett.* **94**, 197601 (2005).
³A. Vasudevarao *et al.*, *Phys. Rev. Lett.* **97**, 257602 (2006).
⁴G. Catalan, J. F. Scott, A. Schilling, and J. M. Gregg, *J. Phys.: Condens. Matter* **19**, 022201 (2007).
⁵C. Kittel, *Phys. Rev.* **70**, 965 (1946).
⁶N. D. Mathur and P. B. Littlewood, *Solid State Commun.* **119**, 271 (2001).
⁷A.-M. Haghiri-Gosnet and J.-P. Renard, *J. Phys. D* **376**, R127 (2003).
⁸D. I. Golosov, *Phys. Rev. B* **67**, 064404 (2003).
⁹M. S. Rzchowski and R. Joynt, *Europhys. Lett.* **67**, 287 (2004).
¹⁰E. Dagotto, T. Hotta, and A. Moreo, *Phys. Rep.* **344**, 1 (2001).
¹¹N. D. Mathur *et al.*, *J. Appl. Phys.* **86**, 6287 (1999).
¹²I. Pallecchi *et al.*, *J. Appl. Phys.* **99**, 114508 (2006).
¹³S. J. Lloyd, N. D. Mathur, J. C. Loudon, and P. A. Midgley, *Phys. Rev. B* **64**, 172407 (2001).
¹⁴A. D. Kent, J. Yu, U. Rüdiger, and S. S. P. Parkin, *J. Phys.: Condens. Matter* **13**, R461 (2001).
¹⁵M. Yamanaka and N. Nagaosa, *J. Phys. Soc. Jpn.* **65**, 3088 (1996).
¹⁶J.-L. Maurice *et al.*, *Appl. Surf. Sci.* **188**, 176 (2002).
¹⁷T. Arnal *et al.*, *J. Magn. Magn. Mater.* **300**, e274 (2006).
¹⁸G.-M. Zhao, H. Keller, W. Prellier, and D. J. Kang, *Phys. Rev. B* **63**, 172411 (2001).
¹⁹M. Bibes *et al.* *J. Phys.: Condens. Matter* **17**, 2733 (2005).
²⁰L. Klein, Y. Kats, A. F. Marshall, J. W. Reiner, T. H. Geballe, M. R. Beasley, and A. Kapitulnik, *Phys. Rev. Lett.* **84**, 6090 (2000).
²¹J. M. D. Coey, M. Viret, L. Ranno, and K. Ounadjela, *Phys. Rev. Lett.* **75**, 3910 (1995).
²²M. Bowen, A. Barthelemy, M. Bibes, E. Jacquet, J. P. Contour, A. Fert, F. Ciccacci, L. Duo, and R. Bertacco, *Phys. Rev. Lett.* **95**, 137203 (2005).
²³U. Ebels, A. Radulescu, Y. Henry, L. Piraux, and K. Ounadjela, *Phys. Rev. Lett.* **84**, 983 (2000).
²⁴T. Kimura, Y. Otani, I. Yagi, K. Tsukagoshi, and Y. Aoyagi, *J. Appl. Phys.* **94**, 7266 (2003).
²⁵M. Kläui, P. O. Jubert, R. Allenspach, A. Bischof, J. A. C. Bland, G. Faini, U. Rudiger, C. A. F. Vaz, L. Vila, and C. Vouille, *Phys. Rev. Lett.* **95**, 026601 (2005).
²⁶A. Thiaville, Y. Nakatani, J. Miltat, and Y. Suzuki, *Europhys. Lett.* **69**, 990 (2005).
²⁷M. Bowen *et al.*, *Appl. Phys. Lett.* **82**, 233 (2003).
²⁸I. Pallecchi, L. Pellegrino, A. Caviglia, E. Bellingeri, G. Canu, G. C. Gazzadi, A. S. Siri, and D. Marre, *Phys. Rev. B* **74**, 014434 (2006).
²⁹H. Y. Hwang, S.-W. Cheong, N. P. Ong, and B. Batlogg, *Phys. Rev. Lett.* **77**, 2041 (1996).
³⁰V. Garcia, M. Bibes, A. Barthelemy, M. Bowen, E. Jacquet, J. P. Contour, and A. Fert, *Phys. Rev. B* **69**, 052403 (2004).
³¹J. M. D. Coey, M. Viret, and S. von Molnár, *Adv. Phys.* **48**, 167 (1999).
³²K. Steenbeck and R. Hiergeist, *Appl. Phys. Lett.* **75**, 1778 (1999).
³³M. Bibes, L. Balcells, S. Valencia, J. Fontcuberta, M. Wojcik, E. Jedryka, and S. Nadolski, *Phys. Rev. Lett.* **87**, 067210 (2001).